Performances of a diode end-pumped GYSGG/Er,Pr:GYSGG composite laser crystal operated at 2.79 μm

Jiakang Chen,[1,2] Dunlu Sun,[1,*] Jianqiao Luo,[1] Huili Zhang,[1,2] Shihao Cao,[1,2] Jingzhong Xiao,[3] Hongxiang Kang,[4] Qingli Zhang,[1] and Shaotang Yin[1]

[1]*The Key Laboratory of Photonic Devices and Materials, Anhui Province, Anhui Institute of Optics and Fine Mechanics, Chinese Academy of Sciences, Hefei, 230031, China*
[2]*University of Chinese Academy of Sciences, Beijing, 100049, China*
[3]*CEMDRX, Physics Department, Universidade de Coimbra, Coimbra, P-3004-516, Portugal*
[4]*Institute of Radiation Medicine, Academy of Military Medical Sciences, Beijing 100850, China*
[*]*dlsun@aiofm.ac.cn*

Abstract: We demonstrate a comparative investigation on Er,Pr:GYSGG and GYSGG/Er,Pr:GYSGG composite crystals at 2.79 μm. Simulating results show the highest temperatures are 369 K and 318 K, respectively. A maximum output power of 825 mW with slope efficiency of 19.2% and maximum laser energy of 3.65 mJ with slope efficiency of 22.7% are obtained in the GYSGG/Er,Pr:GYSGG composite crystal, which have an obvious improvement than those of Er,Pr:GYSGG crystal. The thermal focal lengths are respectively 41 and 62 mm when the pump power is 2.5 W. All these results indicate that the GYSGG/Er,Pr:GYSGG composite crystal has great advantages in reducing the influence of thermal effects and improving laser performances.

OCIS codes: (140.3500) Lasers, erbium; (140.3480) Lasers, diode-pumped; (160.5690) Rare-earth-doped materials.

References and links

1. T. Y. Fan and R. L. Byer, "Diode laser-pumped solid-state lasers," IEEE J. Quantum Electron. **24**(6), 895–912 (1988).
2. A. K. Cousins, "Temperature and thermal stress scaling in finite-length end-pumped laser rods," IEEE J. Quantum Electron. **28**(4), 1057–1069 (1992).
3. Y. T. Chang, Y. P. Huang, K. W. Su, and Y. F. Chen, "Comparison of thermal lensing effects between single-end and double-end diffusion-bonded Nd:YVO_4 crystals for $^4F_{3/2}\rightarrow{}^4I_{11/2}$ and $^4F_{3/2}\rightarrow{}^4I_{13/2}$ transitions," Opt. Express **16**(25), 21155–21160 (2008).
4. B. Neuenschwander, R. Weber, and H. P. Weber, "Determination of the thermal lens in solid-state lasers with stable cavities," IEEE J. Quantum Electron. **31**(6), 1082–1087 (1995).
5. B. Ozygus and Q. Zhang, "Thermal lens determination of end-pumped solid-state lasers using primary degeneration modes," Appl. Phys. Lett. **71**(18), 2590–2592 (1997).
6. F. Song, C. Zhang, X. Ding, J. J. Xu, G. Y. Zhang, M. Leigh, and N. Peyghambarian, "Determination of thermal focal length and pumping radius in gain medium in laser-diode-pumped Nd:YVO_4 lasers," Appl. Phys. Lett. **81**(12), 2145–2147 (2002).
7. F. Hanson, "Improved laser performance at 946 and 473 nm from a composite Nd:$Y_3Al_5O_{12}$ rod," Appl. Phys. Lett. **66**(26), 3549–3551 (1995).
8. R. Weber, B. Neuenschwander, M. M. Donald, M. B. Roos, and H. P. Weber, "Cooling schemes for longitudinally diode laser-pumped Nd:YAG rods," IEEE J. Quantum Electron. **34**(6), 1046–1053 (1998).
9. M. Tsunekane, N. Taguchi, and H. Inaba, "Efficient 946-nm laser operation of a composite Nd:YAG rod with undoped ends," Appl. Opt. **37**(24), 5713–5719 (1998).
10. B. J. Shen, H. X. Kang, D. L. Sun, Q. L. Zhang, S. T. Yin, P. Chen, and J. Liang, "Investigation of laser diode end pumped Er:YSGG/YSGG composite crystal lasers at 2.79 μm," Laser Phys. Lett. **11**(1), 015002 (2014).
11. M. Tsunekane, N. Taguchi, and H. Inaba, "Improvement of thermal effects in a diode-end-pumped, composite Tm:YAG rod with undoped ends," Appl. Opt. **38**(9), 1788–1791 (1999).
12. M. P. MacDonald, Th. Graf, J. E. Balmer, and H. P. Weber, "Reducing thermal lensing in diode-pumped laser rods," Opt. Commun. **178**(4–6), 383–393 (2000).

#221334 - $15.00 USD Received 19 Aug 2014; revised 14 Sep 2014; accepted 15 Sep 2014; published 22 Sep 2014

13. J. K. Chen, D. L. Sun, J. Q. Luo, J. Z. Xiao, H. X. Kang, H. L. Zhang, M. J. Cheng, Q. L. Zhang, and S. T. Yin, "Spectroscopic, diode-pumped laser properties and gamma irradiation effect on Yb, Er, Ho:GYSGG crystals," Opt. Lett. **38**(8), 1218–1220 (2013).
14. D. S. Knowles and H. P. Jenssen, "Unconversion versus Pr-deactivation for efficient 3 μm laser operation in Er," IEEE J. Quantum Electron. **28**(4), 1197–1208 (1992).
15. J. K. Chen, D. L. Sun, J. Q. Luo, H. L. Zhang, R. Q. Dou, J. Z. Xiao, Q. L. Zhang, and S. T. Yin, "Spectroscopic properties and diode end-pumped 2.79 μm laser performance of Er,Pr:GYSGG crystal," Opt. Express **21**(20), 23425–23432 (2013).
16. M. E. Innocenzi, H. T. Yura, C. L. Fincher, and R. A. Fields, "Thermal modeling of continuous-wave end-pumped solid-state lasers," Appl. Phys. Lett. **56**(19), 1831–1833 (1990).
17. J. H. Liu, J. R. Lu, J. H. Lu, Z. S. Shao, and M. H. Jiang, "Thermal lens determination of end-pumped solid-state lasers by a simple direct approach," Chin. Phys. Lett. **16**(3), 181–183 (1999).

1. Introduction

Diode-pumped solid-state laser has been applied widely due to its compactness, reliability, and high efficiency [1]. However, a diode-end-pumped configuration with the smaller laser beam waist, higher density of pump power, and inhomogeneous heating makes thermal lensing effect become a serious problem, which seriously influences the laser stability, achievable maximum average power, efficiency, and so on [2,3]. Therefore, an efficient reduction of thermal lensing effect is significant to promote the laser performance. Some literature reported that the resonant cavity was designed to optimize the laser performance by determining the focal length of thermal lens [4–6]. In recent years, a composite crystal with undoped host as end cap has been regarded as a promising method for cooling the laser crystal and improving the laser performance of diode-pumped solid state laser [7–12]. With the reduction of crystal temperature rise, a more uniform longitudinal temperature distribution can be generated to bring a higher average power. In addition, Er^{3+} serves as an active ion emitting 2.7-3 μm by $^4I_{11/2}\rightarrow{}^4I_{13/2}$ transition, which is commonly believed to be self-terminating because the lifetime of the laser upper level is far less than that of the lower level. An effective method of reducing the lifetime of the lower laser level is the co-doping of deactivation ions [13,14], which is advantageous to population inversion. The Er,Pr:GYSGG crystal has been demonstrated as an excellent laser material for diode-pumped laser at 2.79 μm due to its shorter lower-level lifetime, lower laser threshold and higher laser efficiency [15].

In this work, the concentrations of activation Er^{3+} and deactivation Pr^{3+} ions are further optimized, and a composite GYSGG/Er,Pr:GYSGG crystal is obtained by bonding thermally with undoped GYSGG crystal as end cap in order to reduce the thermal lensing effect. Moreover, we simulate theoretically the thermal induced temperature distribution of the crystals and demonstrate a comparative investigation on laser performance of diode end-pumped Er,Pr:GYSGG and GYSGG/Er,Pr:GYSGG composite crystals operated at 2.79 μm.

2. Experimental details

Our previous experiment results [13,15] showed a high deactivator ions concentration is disadvantageous to the improvement of maximum laser output power. An optimal doping concentration should be able to decrease obviously the laser lower level lifetime, meantime, the laser upper level lifetime has only small decline. Therefore, we choose the optimized concentration by a large number of polycrystalline powder samples with various Er^{3+} and Pr^{3+} doping concentrations. In this work, an Er,Pr:GYSGG crystal was grown from a melt of congruent composition containing optimal doping concentrations (18 at.% Er^{3+} and 0.15 at.% Pr^{3+}) by the Czochralski method. The structural formula can be written as $(Er_{0.54}Pr_{0.0045}Gd_{1.17}Y_{1.2855})Sc_2Ga_3O_{12}$. A pure GYSGG crystal was bonded thermally to Er,Pr:GYSGG at 1200 °C for 10 h. A FLSP 920 fluorescence spectrometer (Edinburgh instrument Ltd, UK) was used to measure the fluorescence spectrum with a 968 nm laser diode (LD) excitation source, and fluorescence decay curves were obtained by excitation with an Opolette 355 I OPO laser (OPOTEK, Inc, USA).

The configuration for generating laser output is shown in Fig. 1. The pump source is an InGaAs LD emitting up to 40 W at around 968 nm in CW and pulse modes. The pump beam

#221334 - $15.00 USD Received 19 Aug 2014; revised 14 Sep 2014; accepted 15 Sep 2014; published 22 Sep 2014

waist diameter in the crystal was approximated to be 100 μm and the fiber core numerical aperture (NA) is 0.15. The dimensions of the Er,Pr:GYSGG and GYSGG/Er,Pr:GYSGG composite crystals are 2 × 2 × 5 mm^3 and 2 × 2 × 7 mm^3 (the doped part Er,Pr:GYSGG is 2 × 2 × 5 mm^3 and the undoped GYSGG is 2 × 2 × 2 mm^3), respectively. The photograph of the GYSGG/Er,Pr:GYSGG composite crystal is shown in Fig. 1. Both faces of the crystals are polished but not anti-reflection (AR) coated. The laser crystal is wrapped in indium foil and mounted between two water-cooled plane-polished copper heat sink. The water temperature was maintained at 12°C. A simple plane–parallel cavity was used as resonator cavity, and the optimized cavity length was 12 mm. A K9 glass plate with antireflection coating of high transmission (HT)>95% at 968 nm and reflectivity of 100% at 2.79 μm was used as the input mirror. The output mirror (CaF_2 substrate) with transmittance of 2% at 2.79 μm was used. The laser output power was measured by a power meter (OPHIR 30A-BB-18) and energy was measured by an energy meter (OPHIR PE50-DIF-C).

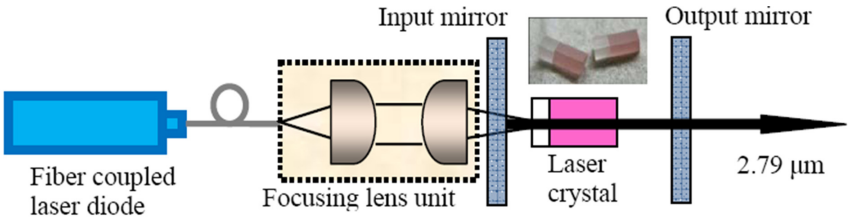

Fig. 1. Schematic diagram of LD end-pumped GYSGG/Er,Pr:GYSGG composite crystal.

3. Results and discussion

In order to better explain the thermal conduction property of composite crystal, based on the thermal conductive modeling [16], the temperature distribution of the LD end-pumped Er,Pr:GYSGG and GYSGG/Er,Pr:GYSGG composite crystals are simulated using mathematical software MATLAB, as shown in Fig. 2, and the relevant parameters are exhibited in Table 1. The highest temperatures in the Er,Pr:GYSGG and GYSGG/Er,Pr:GYSGG composite crystals are 369 K and 318 K, respectively. The center temperature of the GYSGG/Er,Pr:GYSGG composite crystal is much lower than that of the Er,Pr:GYSGG crystal. Efficient heat removing in a composite part can reduce the peak temperature rise in the active segment. This phenomenon is most likely due to the fact that the heat generated in the Er,Pr:GYSGG crystal transfers to the undoped GYSGG crystal, which functions as a heat sink for the pumping surface [11]. In addition, it is worth mentioning that mechanical stresses on the pumped face should appear and create another lens under such high temperature values around 350 K. This effect may be low compared to the thermal lens but it could not be ignored. Therefore, further studies may focus on how to decrease the mechanical stresses on the pumped face by theoretical and experiment works.

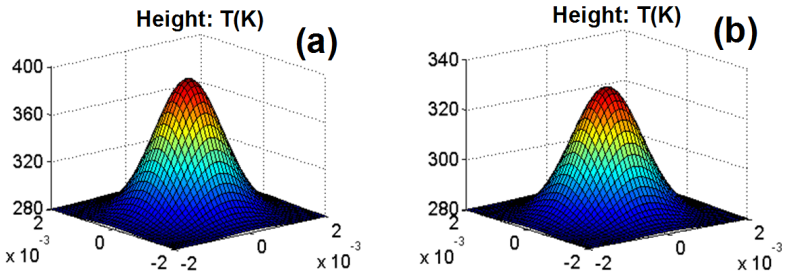

Fig. 2. Temperature distribution on the pump end-face of the crystals. (a) Er,Pr:GYSGG; (b) GYSGG/Er,Pr:GYSGG.

#221334 - $15.00 USD Received 19 Aug 2014; revised 14 Sep 2014; accepted 15 Sep 2014; published 22 Sep 2014

Table 1. Parameters of the temperature distribution simulating.

Thermal conductivity (κ)	4.663 W/(m·K)
Input power (P_{in})	3 W
Absorption coefficient (α)	3.8 cm^{-1}
Heat transfer coefficient (h)	0.4
Radius of pumping faculae (ω_p)	100 μm
Temperature of heat sink (T)	285.2 K
Length of crystal (d)	5 mm

The fluorescence spectrum of the Er,Pr:GYSGG crystal excited by a 968 nm LD is shown in Fig. 3. Three strongest fluorescence peaks (2637, 2703, and 2793 nm) are observed within 2.6–3 μm, which result from the transitions of stark sub-levels from $^4I_{11/2}$ to $^4I_{13/2}$. The OPO-excited fluorescence decay curves of 1.016 and 1.530 μm show a single exponential decay behavior. The lifetimes of the upper level $^4I_{11/2}$ and lower level $^4I_{13/2}$ are fitted to be 0.69 and 0.86 ms, respectively (Fig. 4). By contrast, the lifetimes of the upper level $^4I_{11/2}$ and lower level $^4I_{13/2}$ are 0.52 and 0.60 ms in our early Er,Pr:GYSGG crystal doped with 20 at.% Er^{3+} and 0.3 at.% Pr^{3+} [15]. Both the lifetime ratios between the $^4I_{13/2}$ and $^4I_{11/2}$ for the two crystals are close to 1.2. However, the upper level lifetime of the present Er,Pr:GYSGG crystal (0.69 ms) is longer than that of pervious one (0.52 ms), which should be more favorable to energy storage during diode continuous wave (CW) pumping. Therefore, it is believed that the present Er,Pr:GYSGG crystal with optimized doping concentrations should have more excellent laser performance.

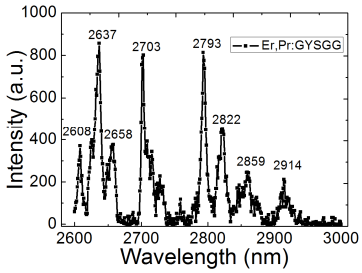

Fig. 3. Fluorescence spectrum of Er,Pr:GYSGG crystal excited by a 968 nm LD.

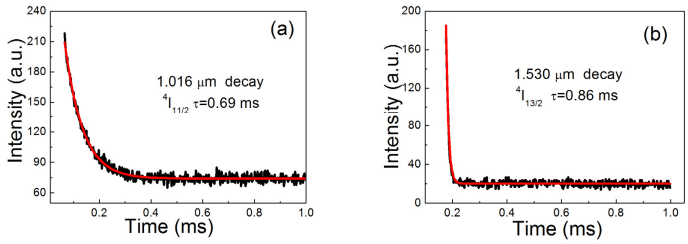

Fig. 4. Fluorescence decay curves (a) at 1.016 μm and (b) 1.530 μm.

Figure 5 shows the laser output power as a function of input pump power for Er,Pr:GYSGG and GYSGG/Er,Pr:GYSGG composite crystals. The pump laser is operated in the CW mode, and the cavity length is maintained at an optimized length 12 mm for both crystals. The output coupler with a transmission of 2% is applied according to our previous work [15]. For the Er,Pr:GYSGG crystal, a maximum laser power of 430 mW corresponding to the threshold of 102 mW is obtained. Linear fitting results show the optical-to-optical efficiency is 17.0% and slope efficiency is 17.7%. However, under the same conditions, a maximum laser power of 825 mW, the threshold of 90 mW, optical-to-optical efficiency of 18.7% and slope efficiency of 19.2% are achieved in the GYSGG/Er,Pr:GYSGG composite

#221334 - $15.00 USD Received 19 Aug 2014; revised 14 Sep 2014; accepted 15 Sep 2014; published 22 Sep 2014

crystal. At 150 mW output power, the far-field divergence of 6.2/6.0 mrad and M^2 factor of 1.74/1.71 were determined using the knife-edge method in non-composite/composite crystals, respectively. These results should mainly due to the fact that the heat generated in the Er,Pr:GYSGG crystal transfers to the undoped GYSGG crystal, which functions as a heat sink for the pumping surface [11]. Thus, the surface deformation and thermal lensing effects are massively reduced, and the properties of laser output are greatly improved in the GYSGG/Er,Pr:GYSGG composite crystal.

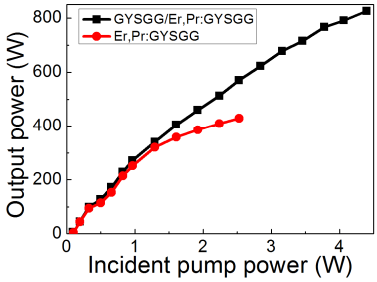

Fig. 5. Output power versus pump power for the two crystals.

In addition, we can find another fact that the laser output of the conventional Er,Pr:GYSGG crystal is better than our previous work under the same conditions [15]. A maximum laser power of 284 mW, threshold of 112 mW, and slope efficiency of 17.4% were obtained in our early Er,Pr:GYSGG crystal. The laser performance improvement of the present Er,Pr:GYSGG crystal indicates that the optimized concentration of 18 at% Er^{3+} and 0.15 at % Pr^{3+} is more advantageous to generate laser.

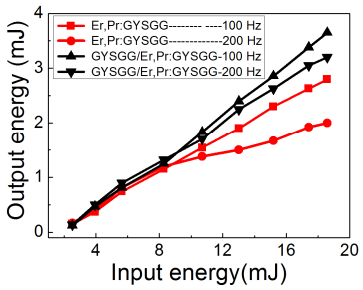

Fig. 6. Output energy versus input energy for different repetition rates on the two crystals.

The output energy gained from the Er,Pr:GYSGG and GYSGG/Er,Pr:GYSGG composite crystals with different repetition rates of 100 and 200 Hz are exhibited in Fig. 6. Meanwhile, output couplers with 2% transmission, pulse duration with 0.5 ms and 12 mm-long cavity were used throughout the entire experiment. When the repetition rate is maintained at 100 Hz for the Er,Pr:GYSGG crystal, a maximum laser energy of 2.82 mJ is obtained, corresponding to a peak power of 5.6 W. Linear fitting results show an optical–optical conversion efficiency of 17.8% and a slope efficiency of 20.1%. For the GYSGG/Er,Pr:GYSGG composite crystal, a maximum laser energy of 3.65 mJ is obtained, corresponding to a peak power of 7.3 W. Linear fitting results show an optical–optical conversion efficiency of 19.6% and a slope efficiency of 22.7%. Notably, the laser performance of the GYSGG/Er,Pr:GYSGG composite crystal is higher than that of the Er,Pr:GYSGG crystal. In addition, the output energy drops when the repetition rate at 200 Hz. However, for the GYSGG/Er,Pr:GYSGG composite crystal, the dropping extent of the laser energy at high repetition rate is much more slightly than that of the Er,Pr:GYSGG crystal. These results further explain that the thermal lensing

#221334 - $15.00 USD Received 19 Aug 2014; revised 14 Sep 2014; accepted 15 Sep 2014; published 22 Sep 2014

effects can be effectively reduced when the undoped GYSGG is bonded to the Er,Pr:GYSGG crystal, and the laser performance of the composite crystal can be improved obviously.

In order to further illustrate the influence of GYSGG/Er,Pr:GYSGG composite crystal on the thermal lensing effect, the thermal focal lengths of the two crystals were measured. According to the conditions of stable cavity [17]:

$$0 < (1 - L_c / f_T)(1 - L_c / R) < 1 \quad (1)$$

where f_T is the thermal focal length of the crystal, R is the curvature radius of the flat mirror ($1/R = 0$). Thus, $L_c < f_T$ should be maintained in order to keep the resonator cavity stable. When we move the output mirror to render $L_c > f_T$, the output power would decrease to zero, and the resonator cavity will be metastable at $L_c = f_T$. Therefore, the thermal focal length of the crystal can be obtained by moving the output mirror to make the output power equal to zero when the pump power maintain a determining value.

Figure 7 shows the thermal focal lengths of the Er,Pr:GYSGG and GYSGG/Er,Pr:GYSGG composite crystals measured by the approach described above. The thermal focal length of the GYSGG/Er,Pr:GYSGG composite crystal is 62 mm when the pump power is 2.5 W, while the thermal focal length of the Er,Pr:GYSGG crystal is only 41 mm under the same conditions. These results fully demonstrate that the deformation of pump surface and refractive index change of GYSGG/Er,Pr:GYSGG composite crystal are much smaller than those of the Er,Pr:GYSGG crystal, and the thermal lensing effects can be effectively reduced.

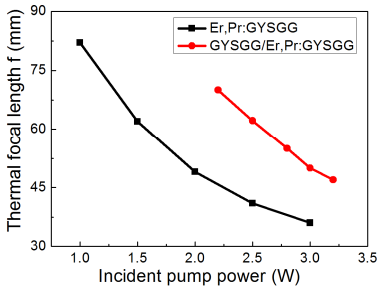

Fig. 7. Thermal focal lengths of laser crystals as a function of pump power.

4. Conclusions

The Er,Pr:GYSGG crystal with optimized doping concentrations of activation Er^{3+} and deactivation Pr^{3+} ions was bonded thermally with undoped GYSGG crystal. The highest temperatures in the Er,Pr:GYSGG and GYSGG/Er,Pr:GYSGG composite crystals are simulated to be 369 K and 318 K, respectively. The maximum laser output powers of the two crystals are 430 mW and 825 mW, which correspond to slope efficiencies of 17.7% and 19.2%, and laser thresholds of 102 mW and 90 mW, respectively. The maximum laser output energies of the two crystals are 2.82 mJ and 3.65 mJ, which correspond to peak powers of 5.6 W and 7.3 W, slope efficiencies of 20.1% and 22.7%, respectively. The thermal focal lengths are measured to be 41 mm and 62 mm for the two crystals when the pump power is maintained at 2.5 W. All these results suggest that the GYSGG/Er,Pr:GYSGG composite crystal has great advantages in reducing thermal effects and improving laser performances, and a composite end cap is a suitable cooling structure for efficient and high-power operation of diode end-pumped solid-state lasers.

Acknowledgments

This work was supported by the National Natural Science Foundation of China (Grant Nos. 91122021, 51272254, 61205173, and 51172236).

#221334 - $15.00 USD Received 19 Aug 2014; revised 14 Sep 2014; accepted 15 Sep 2014; published 22 Sep 2014